# Optimizing Shared Mooring and Anchoring Strength for Floating Offshore Wind Turbine Arrays

by
Michael C Devin

A THESIS

submitted to

Oregon State University

Honors College

in partial fulfillment of
the requirements for the
degree of

Honors Baccalaureate of Science in Mechanical Engineering
(Honors Scholar)

Presented March 5, 2019
Commencement June 2019

# AN ABSTRACT OF THE THESIS OF

Michael C Devin for the degree of Honors Baccalaureate of Science in Mechanical Engineering presented on March 5, 2019. Title: Optimizing Shared Mooring and Anchoring Strength for Floating Offshore Wind Turbine Arrays

.

Abstract approved:_____

Bryony DuPont

Energy from offshore wind could provide substantial power generation if further utilized. One area of significant research focus is in developing floating offshore wind devices, which would allow for wind energy to be gathered in deep water where driven monopile turbines are infeasible. However, floating offshore wind is not currently marketable, and design optimization is required for it to approach financial viability. A method proposed to decrease the cost is to connect mooring lines from multiple turbines to a single anchor. The dynamics of this system are complex and decrease the reliability of the components of the wind array. A proposed hypothesis to remedy this is to strengthen a small number of important anchors significantly more than the rest. A noise-resistant optimization algorithm was developed using elements of genetic algorithms and Bayesian optimization to identify the optimal anchors to strengthen to improve safety. A previously developed simulation that evaluates the reliability of a hypothetical floating wind array utilizing the multi-line anchor concept was used as an objective function. While the resultant reliability values were uncompetitive compared to slightly strengthening all anchors, analyzed trends showed opportunity for the concept to work if a higher number of anchors are overstrengthened.

Key Words: optimization, renewable, wind, marine, energy
Corresponding e-mail address: michaelcdevin@outlook.com

# Optimizing Shared Mooring and Anchoring Strength for Floating Offshore Wind Turbine Arrays

by
Michael C Devin

A THESIS

submitted to

Oregon State University

Honors College

in partial fulfillment of
the requirements for the
degree of

Honors Baccalaureate of Science in Mechanical Engineering
(Honors Scholar)

Presented March 5, 2019
Commencement June 2019

Honors Baccalaureate of Science in Mechanical Engineering project of Michael C Devin presented on March 5, 2019.

APPROVED:

_____

Bryony DuPont, Mentor, representing Mechanical Engineering

_____

Pedro Lomónaco, Committee Member, representing Civil Engineering

_____

Matthew Campbell, Committee Member, representing Mechanical Engineering

_____

Toni Doolen, Dean, Oregon State University Honors College

I understand that my project will become part of the permanent collection of Oregon State University, Honors College. My signature below authorizes release of my project to any reader upon request.

_____

Michael C Devin, Author

# Acknowledgements

To Sanjay Arwade and Spencer Hallowell, for planting the ideas that became the crux of my research, and for your insight as my research neared its end.

To Caity Clark, for bringing up RBDO as a potential solution just as I thought I was reaching a dead end.

To my roommates, Nathan DeStafeno and Aaditya Kumar, for not only making sure I still laugh even in the face of frequent stress, but also for tolerating my incessant yelling at my computer as I tried to get my code to work.

To Mom and Dad, for your relentless support, encouragement, and advice.

And to Bryony DuPont – I have had such a privilege to work with such a fantastic mentor and a fantastic person. I'm looking forward to continuing to work with you as I pursue graduate school.

# Table of Contents

# Chapter 1: Introduction

With the continuously increasing power consumption of the United States, new sources of energy must be found for sector growth to continue. Total national energy production is estimated to increase by more than 20% by 2040, largely from an increase in power generation from natural gas and renewable sources [1]. One area of significant potential in energy production lies with offshore wind energy. Offshore wind energy has 4,150 GW of potential power capacity in the United States, almost four times the power capacity from all energy sources as of 2016 [2]. Due to higher and more consistent wind speeds, the resource potential per area for offshore wind is significantly higher than onshore sites. In particular, the southern Oregon coast and northern California coast has a wind power density of more than 800 $W/m^2$, the highest resource area in the contiguous United States [3].

While large offshore wind farms already exist – particularly in northern Europe [4] – the potential of offshore wind is being limited by current methods of turbine installation. Almost all offshore wind farms in commercial operation use a fixed foundation, using a driven-monopile underwater structure, where the base of the turbine is driven directly into the seabed in a manner analogous to land-based turbines. However, this method of installation becomes impractical and prohibitively expensive at depths greater than 30 meters due to practical limitations of building monopiles tall enough. Particularly off the west coast of North America, the gradient of the sea bed is so steep that offshore turbines cannot be practically installed this way due to the ocean depth [5]. Additionally, deeper waters – beyond the point where pile-driven wind turbines can be installed – typically allow for steadier, stronger winds, as well as being politically less problematic due to the decreased conflict with shipping lanes, fishing areas, and coastal land owners.

To take advantage of this wind resource, floating offshore wind is an area of significant focus. Floating offshore wind turbines (FOWTs) consist of the wind turbine buoyed on a floating platform, with several mooring cables connecting the floating platform to anchors embedded in the ocean floor. There are many types of platforms, anchors, and cables being considered for different situations and costs, as outlined in Table 1. Floating offshore wind turbines have been demonstrably shown to be functionally viable in simulations, full-scale prototypes, and in Hywind Scotland, the world's first commercial floating wind farm [6]. However, offshore wind is still too expensive to be commercially viable on a widespread scale. According to a capital expenditure report prepared for the Scottish government in 2015, the cost for a single 6 MW floating wind prototype was about £5.2m/MW, far above the £3m/MW limit estimated for commercial deployment. To reduce the costs for this, significant optimization needs to be conducted for all components of the design for FOWTs. While a large percentage of the cost reduction needs to be done via optimizing the turbine platform (which falls outside the scope of this research), 4% of the cost reduction is expected to come from the optimization of the anchors and mooring for the FOWT [7].

**Table 1.** List of various parameters undergoing significant research for floating offshore wind turbines.

| Platform | Anchor | Mooring material | Mooring orientation |
|---|---|---|---|
| • Semi-submersible<br>• Spar buoy<br>• Tensioned-leg platform (TLP) | • Plate anchor<br>• Gravity anchor<br>• Pilot<br>• Drag embedment anchor | • Chain<br>• Cable<br>• Fiber | • Catenary<br>• Transitional<br>• TLB (diagonal)<br>• TLP (perpendicular) |

One hypothesized method to optimize mooring and anchors for FOWTs is to utilize shared mooring or anchors. In a typical array of FOWTs, each turbine has its own set of mooring lines, with a single mooring line connecting to a single anchor. For a shared mooring or anchor configuration, a turbine shares mooring lines and anchors with some or all of the adjacent

turbines. The cost benefits from such a system also increase as the size of a wind farm grows. While many methods exist to connect shared mooring and cables, all methods significantly reduce the length of mooring lines and the number of anchors needed in an array of FOWTs.

# Chapter 2: Previous Approaches

## 2.1 Anchor and Mooring Optimization

Significant research exists for optimizing standard mooring and anchoring for FOWTs. Molins et al. used a derivative-based optimization algorithm to optimize the design of a catenary mooring system for a scaled spar buoy platform based on the weight of the mooring lines [8]. Brommundt et al. introduced a tool for optimizing catenary mooring system for semi-submersible FOWT platforms by minimizing the total mooring length to reduce cost using direct search methods [9]. This model takes into account both normal and worst-case environmental loadings over the life cycle of a FOWT using frequency domain analysis to determine the linear response of the platform. Chen et al. performed mooring optimization with similar methods for a FOWT with a spar buoy platform [10], and Benassai et al. has accomplished the same with chain cable catenary mooring lines for a candidate platform location in the southern Tyrrhenian Sea [11].

Fylling has created an automated optimization method using a computer program MOOROPT to minimize mooring and riser material costs for general floating systems using derivative-based optimization [12], later expanding the work specifically for FOWTs by developing WINDOPT [13]. While initially only including the number of mooring lines, riser lines, maximum loads, and fatigue constraints as parameters, WINDOPT expanded to include

parameters regarding the turbine dimensions, aerodynamic forces, and specific dimensions of a spar buoy platform.

While these approaches have established the foundation for future research efforts, none of these works explore optimizing shared mooring.

## 2.2 Multiline Modeling

Shared mooring and anchor systems are a relatively new development, and concepts have only been independently developed with no academic consensus formed on which methods to pursue commercially. Hall has done significant research in quantifying the dynamic modeling of shared mooring lines for FOWTs [14] [15] as well as wave energy converters (WECs), with both Vissio et al. [16] and Sirnivas et al [17]. He has contributed significant effort towards the usage of MoorDyn, a lumped-mass formulation of dynamic modeling for mooring lines [18]. Of particular note, he and Connelly have researched the feasibility of a wind farm configuration where mooring lines are connected directly between platforms, as well as performed dynamics on such a system using FAST and MoorDyn [19].

Goldschmidt and Muskulus investigated a row, triangular, and rectangular configuration of coupled mooring systems and their associated costs and dynamics. The row arrangement in particular is analyzed in the time domain with the estimated effects of aerodynamics caused by the wind and wave forces [20].

Finally, Fontana et al. developed a “multiline” mooring configuration where each anchor moors lines from several FOWTs. These researchers also performed FAST analyses on a theoretical wind farm utilizing multiline anchors. In particular, these works analyze the different

anchor types that would work with this configuration most effectively, as the conceived multiline anchor setup requires the anchors to handle multidirectional loads [21].

## 2.3 Bayesian Optimization

One class of derivative-free optimization is Bayesian optimization. This method is frequently used for evaluations that are computationally expensive. Bayesian optimization is typically formed by two main components: a statistical model where every combination of solutions has a normal distribution (called Gaussian process regression), and an acquisition function that selects where to sample. The Gaussian process is applied to an unknown function before evaluation (called a *prior*) that reflects the expected behavior of the function, often heuristically determined. After the function is evaluated at a set of points (often randomly selected), the results are treated as data, and is used to both update the prior and also to inform the acquisition function as to the best location to evaluate the function in the next iteration [22].

The inclusion of Gaussian process regression allows Bayesian optimization to solve optimization problems that have evaluations with normally-distributed noise, separating it from many other optimization methods. In particular, Bayesian optimization has been historically used for designing engineering systems, where noise is inherent due to physical effects that are uncertain and complex to evaluate precisely, such as stress and fatigue [23]. One application of this is through reliability-based design optimization (RBDO), where the uncertainty of the failure criteria of a system is analyzed and design decisions for the system are made based on Bayesian modeling and optimization [24]. In RBDO, the Gaussian process prior is the expected failure rate of a particular aspect of the analyzed system. Since failure rates are frequently expressed

probabilistically instead of as an explicit value, an optimized solution is still achievable with RBDO due to the tolerance of stochastic noise inherent to Bayesian optimization.

### 2.4 Overall Findings

Overall, at time of writing, the dynamic modeling of a single FOWT is well-developed and widely available. Additionally, there is significant research in optimizing various aspects of a single FOWT. The dynamic modeling for shared mooring and anchor systems is quickly developing, particularly with the aforementioned work of Hall, Fontana, and others. However, little research has been performed regarding optimization of shared mooring and anchor systems for wind farms, which this paper aims to address.

## Chapter 3: Problem Formulation

### 3.1 Hypothesis

The optimization scheme outlined in this paper is based on the same multiline configuration for shared mooring and anchors generated in previous research done by Fontana et al. In particular, this paper expands on the wind farm geometry by having a single anchor moor three OC4 / DeepCWind semisubmersible platforms supporting a standard NREL 5 MW turbine. A detailed visual depiction of the setup is shown in Figure 1. The mooring lines are catenary mooring lines with specifications, listed in Table 2, identical to that of the previous work done by the aforementioned authors.

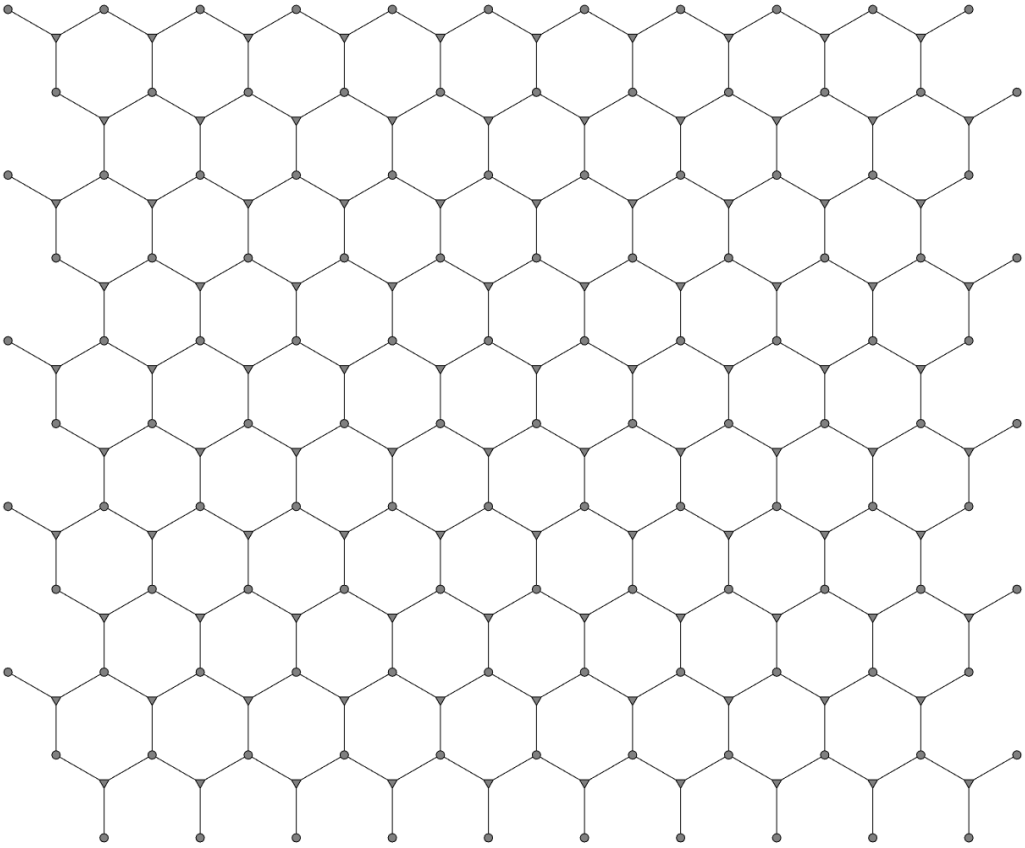

**Figure 1.** Configuration of the analyzed floating offshore wind array. Circles indicate anchors, triangles indicate turbines, and lines indicate mooring lines.

**Table 2.** Parameters of the analyzed floating offshore wind array. These are identical to the parameters used in previous work by Fontana et al.

| **Parameters of Analyzed Floating Offshore Wind Array** | |
|---|---|
| Ocean depth | 200 meters |
| Unstretched mooring line length | 835 meters |
| Mooring line seafloor lay length | 243 meters |
| Radial distance from fairleads to anchors | 797 meters |
| Radial distance from center of platform to fairleads | 41 meters |
| Mean wind speed | 11.4 m/s |
| Turbulence intensity | 0.11 |
| Wave height | 4 meters |
| Peak spectral wave period | 7.1 seconds |

The previous literature from Fontana et al. identified that the multiline concept could reduce the number of anchors in a wind farm by a factor of three, if the anchors used can handle multi-directional loading. However, a further finding of the research – untested at the time – was that the dynamics of such a system would result in complex loading on the anchors due to the complicated coupling involved, which leads to decreased system reliability due to an increased risk of cascading turbine failures [25]. To counteract this decreased reliability, stronger anchors are required, which introduces a cost increase that could eliminate any benefit gained from cutting the number of anchors in the first place.

However, it is possible that the complex dynamics caused by the coupling could actually provide a benefit; it has been hypothesized that having a small number of specific anchors strengthened a large amount would provide better reliability and/or be less expensive than strengthening all of the system anchors a small amount.

To receive the greatest benefit from this hypothesis, the specific anchors – and the amount the anchors are strengthened beyond the "standard" strength in the system (henceforth referred to as "overstrength") – needs to be optimized. Determining the optimal anchors in a specific setup of this multiline anchor configuration (specified in section 3.2), how much they should be overstrengthened, and whether this provides a significant improvement to reliability versus strengthening the entire system a small amount, are the primary goals of this paper.

## 3.2 Objective Function and Simulation Description

The objective function of the problem being addressed is to maximize the reliability of an array of FOWTs, utilizing the multiline anchor scheme with a predetermined number of overstrengthened anchors, as discussed above. "Reliability" in this context is a unitless index

factor representing the mean return period to failure of the array, typically falling between 1 and 2. The reliability of a particular array configuration is determined using a set of MATLAB functions created to evaluate this system[1]. These MATLAB functions first create the general geometric layout of the turbine platforms and the anchors for the array, including the number of rows and columns, the number of turbines and anchors, the number of simulations, and the spacing between turbines. Several sets of data from previous FAST analyses are loaded. These datasets specify the forces from the wind and waves from a specific direction, the wave surge and sway from the given wave direction, and the calculated anchor and mooring line demands from multiple simulations. For the sake of this evaluation, the direction was set to 0º, due north. The simulation also accounts for the positioning displacements of the platforms due to wave surge and sway.

The simulation then configures a wind farm with a consistent geometry. Using the multiline concept previously detailed, the simulation uses an array consisting of 120 anchors and 100 turbines, as shown in Figure 1. The farm is set up in a hexagonal design with all turbines beginning in specific locations at regular intervals, with 10 turbines per row and 5 per column, each turbine separated by 1,450.8 meters in single rows and 2,512.8 meters in single columns. Adjacent rows and columns are offset by half of the distance between turbines within the same row. Each anchor has lines connecting from three different turbines (unless the anchor is on the edge of the array), initially at 120 degrees apart. The base anchor strength (before any overstrengthening) is set at 3460 MPa, and the mooring line strength is 5111 MPa.

Once the geometry and maximum loads are set, the simulation determines the demands on all lines and anchors by sampling the demands from the loaded FAST data on a lognormal

[1] The MATLAB functions used as the evaluation function, as well as the associated loading data, was provided by Spencer Hallowell and Sanjay Arwade of the University of Massachusetts, Amherst.

distribution. If the strength capacity of any line or anchor is less than the demand for that component, it fails, and the function changes the anchor capacity and demands for the surrounding anchors as a result of the failure. The simulation makes use of various other subfunctions to determine these failures, their effects, and the resulting change in demands. Once determined, the simulation runs again to determine if more failures occur as a result of the changes, and the process repeats. The simulation runs until every anchor and turbine has a demand less than its capacity. The entire process is then repeated 5000 times.

At this point, the simulation determines which turbines fail each simulation ("fail" meaning any of the adjacent anchors also failed). The reliability value for the configuration is determined by:

$$\text{Reliability} = -\Phi[1 - (1 - n_{turbinefail1})(1 - n_{turbinefail2})(1 - n_{turbinefail3})]$$

where Φ is the cumulative distribution function of the standard normal distribution, and $n_{turbinefail1}$, $n_{turbinefail2}$, and $n_{turbinefail3}$ are total failure rates of all turbines at each of the three anchor connection points. More specifically,

$$n_{turbinefailx} = \frac{\left(\frac{\text{Total anchor failures at connection point } x}{\text{Total number of turbines}}\right)}{\text{Total number of simulations}}$$

## 3.3 Optimization Algorithm

To find the maximum reliability and the optimal anchors to overstrengthen in this optimization problem, a binary genetic algorithm (GA) was used as the basis of the overall optimization algorithm. However, due to a significant amount of stochastic noise in the

generated solutions created by the sampling of the FAST data in the evaluation, using only a GA failed to converge to an optimal solution (see Section 4.1). The stochastic noise combined with the very large number of potential configurations (about 116 trillion if overstrengthening 10 anchors) necessitated a unique hybrid optimization scheme that introduces elements of Bayesian optimization common in RBDO applications, and an inter-test archive of existing solutions.

### 3.3.1 Binary Genetic Algorithm Elements

In the algorithm, overstrengthened anchors are denoted as 1, while normal strength anchors are denoted as 0. The algorithm takes the number of overstrengthened anchors per array ($n_{OSanchors}$) and the overstrength factor (i.e. the multiplier placed on the anchor strength of the selected overstrengthened anchors) as inputs, with the best reliability value and the corresponding overstrengthened anchors as outputs. The anchor numbering begins in the southeast corner of the array and proceeds north, returning to the southern end of the next column of anchors to the west. At the start of the optimization process, a population is generated with $n_{OSanchors}$ randomly selected overstrengthened anchors in each chromosome. The simulation discussed in the previous section is used as the fitness function, which evaluates each configuration of overstrengthened anchors and outputs a reliability value.

After sorting the solutions by reliability value and the corresponding arrays from best to worst, the best reliability is evaluated. If it is better than the existing best reliability, this value is overwritten, and the new best set of overstrengthened anchors is saved.

The fittest 20% of each set of solutions have their traits cloned directly to the next generation. This high cloning rate is used to decrease stochasticity and decrease the time to convergence.

The process of selection begins with a kill of all below-average chromosomes. The remaining solutions are normalized as follows:

$$\text{Normalized reliability of array } j = \frac{\text{Reliability of array } j - \text{Mean reliability}}{\sum_{i=1}^{n}(\text{Reliability of array } i - \text{Mean reliability})}$$

where *n* is the number of above-average arrays. This normalization is done to exaggerate good solutions, as the range of reliability values within a population was relatively small (typically 0.05 or less), to which selection was sensitive.

Selection was accomplished by ordering the normalized reliability values linearly, then randomly selecting a value within the range of normalized reliabilities. For crossover, instead of using a crossover point, a random permutation of the overstrengthened anchors from the selected parents that match the inputted number of overstrengthened anchors is selected. 60% of the solutions for the following generation consisted of children.

The remaining 20% of chromosomes for the following generation were randomly generated in the same manner as the first generation. This was done because having all chromosomes be composed entirely of children resulted in convergence to local maxima instead of a globally optimal solution.

This optimization process iterates for 100 iterations. At the conclusion of the last iteration, the algorithm outputs the best overall reliability and the corresponding set of overstrengthened anchors.

The determined parameters of the GA formulation, as well as grounds for the selection of each parameter value, are included in Table 3.

**Table 3.** GA parameters, selected values, and rationale for selecting each value.

| **Binary Genetic Algorithm Parameters** | | |
|---|---|---|
| **Parameter** | **Value** | **Grounds** |
| Iteration Limit | 100 | Smaller values led to worse solutions; larger values did not converge any further |
| Population size | 100 | Smaller values led to worse solutions; larger values did not converge any further |
| Number of overstrengthened anchors | 10 (typical) | Selected a small enough number to where the most important anchors would be obvious, but a large enough value to where configuration trends and patterns could be identified. |
| Crossover percentage | 60% | Smaller values do not converge; larger values quickly converge to local maxima |
| Cloning percentage | 20% | Smaller values converge too slowly; larger values converge quicker, but to local maxima |
| Mutation percentage | 0% | Stochasticity in evaluation prevents further stochasticity from being required |

### 3.3.2 Bayesian Optimization Elements

In order to combat the stochastic noise resulting in a lack of convergence when optimizing with a binary GA, elements of Bayesian optimization were added to the algorithm. As discussed earlier, Bayesian optimization is tolerant to stochastic noise, making it suitable for this optimization problem. For this problem, the normal distribution of the reliability results from the evaluation simulation takes the form of the Gaussian process prior of a Bayesian optimization problem. The typical evaluation step in a GA is thus replaced by a Bayesian evaluation process.

Specifically, the evaluation process now takes the following form:

1. The set of overstrengthened anchors for a given solution is read into the program.
    a. If the exact permutation of overstrengthened anchors has not been evaluated before, the simulation evaluates the reliability of that solution 25 times, then calculates and saves the mean reliability for that permutation of overstrengthened anchors.

   b. If the exact permutation of overstrengthened anchors has been previously evaluated, the previously saved mean reliability is extracted, and the simulation evaluates the reliability an additional time. The mean is then recalculated and saved for that permutation of overstrengthened anchors, overwriting the previously saved mean.

2. Each permutation of overstrengthened anchors encountered, the corresponding reliability values, and the corresponding number of times a permutation was evaluated, are each saved in ordered arrays to be referenced in future iterations.

This evaluation process was tested in isolation with five randomly selected sets of overstrengthened anchors, each evaluated for 250 iterations, then repeated four additional times. As shown in Figure 2, the noise associated with the evaluated reliabilities decreases significantly as the number of evaluations increases. The results of this initial test showed that the standard deviation of the reliability values had dropped below 0.001 for all tested overstrengthened anchor solutions by 25 iterations, as shown in Figure 3. Therefore, as discussed in the new evaluation process above, the optimization algorithm evaluated each new solution 25 times. Note that this decision disregards the temporary increase of the black line back above the 0.001 standard deviation mark. The benefits gained from increasing the number of initial tests to 40+ were assumed to be marginal compared to the increase in computational expense.

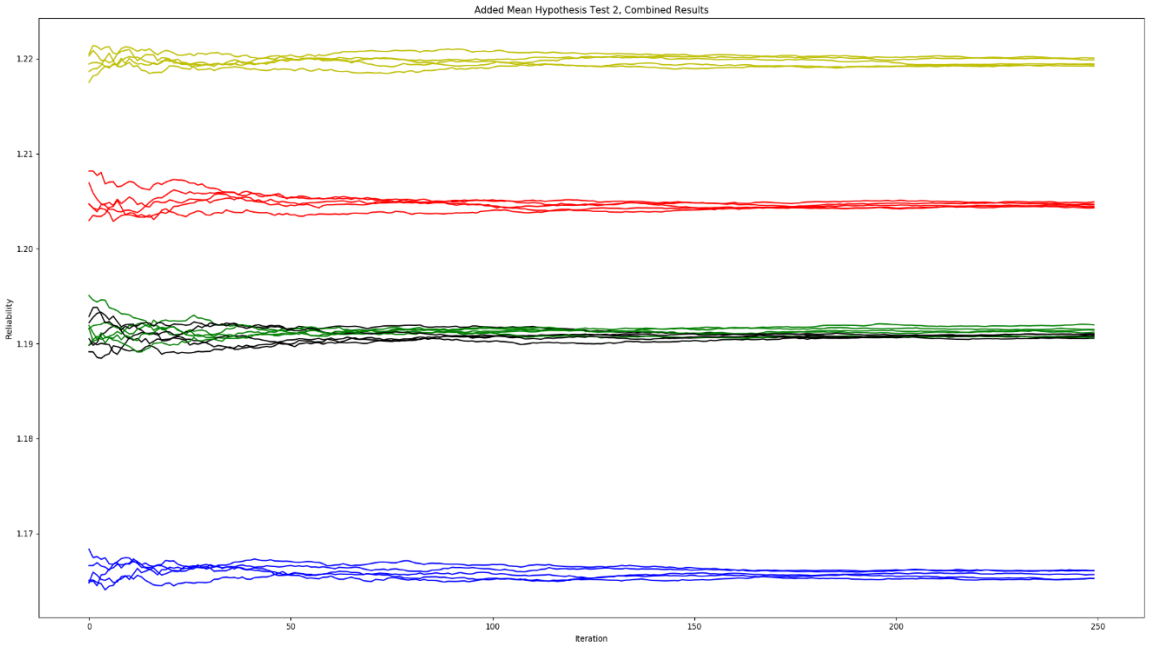


**Figure 2.** Results from running modified evaluation process five times for five different sets of overstrengthened anchors (each set indicated by a different color).

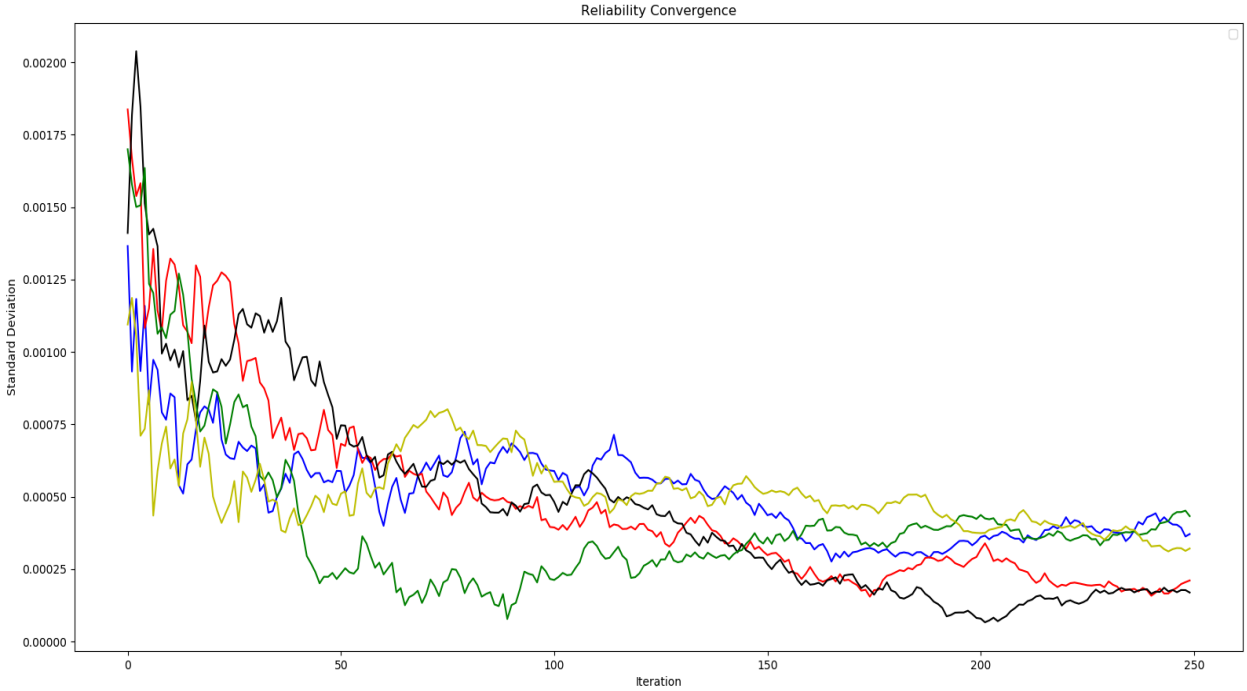


**Figure 3.** Standard deviation vs. Iteration Count for the five sets of overstrengthened anchors in Figure 2.

The cloning, selection, and crossover from the GA elements of the optimization algorithm act as the acquisition function of the algorithm from a Bayesian perspective, thus satisfying the two main components of a Bayesian optimization algorithm.

### 3.3.3 Solution Archiving

Due to the very large number of permutations of overstrengthened anchors, an archive of CSV files was established to save the arrays of overstrengthened anchor configurations, corresponding reliabilities, and the number of tests done for each configuration. These CSV files would be retrieved and read into the optimization algorithm each time it ran, effectively creating a running archive of all configurations that have been tested by the optimization algorithm throughout all of the times it has ever ran (within the specified directory). As the optimization algorithm was tested increasingly more, the archive saved an increasing amount of computation time.

# Chapter 4: Results and Discussion

## 4.1 Initial Results

As previously mentioned, the initial results of the optimization scheme when the algorithm was exclusively a GA failed to result in an optimal solution or convergent behavior. The behavior seen consistently showed the solution improving for approximately 10 iterations before plateauing to a non-convergent value (i.e. the “plateau” reliability would be significantly different with every test). This behavior persisted regardless of the number of iterations the algorithm ran, the population size or crossover percentage used, or the method of crossover used.

As shown in Figure 4, after initial improvements to the reliability, the best reliability found in each iteration would vary drastically, with a new overall best reliability seeming to be found merely by chance, with the 50$^{th}$-percentile and worst reliabilities showing no convergent behavior.

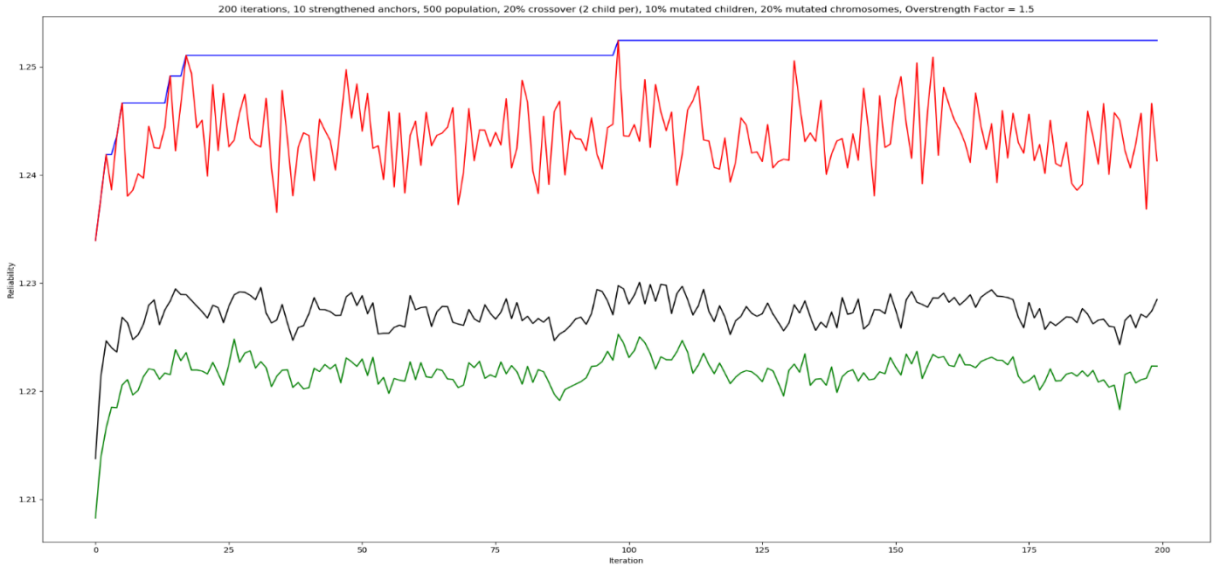


**Figure 4.** Iteration vs. Reliability for the GA-only optimization algorithm. The blue line indicates overall best reliability, the red line indicates iteration-best reliability, the black line indicates reliability of the 50$^{th}$ percentile of each iteration, and the green line indicates iteration-worst reliability. Note the lack of convergence between iteration-best reliabilities.

Despite improvements to the GA that were meant to reduce stochastic behavior, the evaluation itself was found to be the cause of the stochastic results. The probabilistically determined selection of anchor loads from the FAST analyses creates a small amount of noise in the simulation. However, the GA is highly sensitive to noise for this problem, as even minor variations in calculated reliability prevented convergence. The remaining stochasticity is further emphasized in Figure 5, which shows a single configuration evaluated 500 times, with an apparent Gaussian distribution over a reliability range of about 0.04, which is a similar range to the range of reliabilities within a first-generation population in the optimization algorithm. The noise in the simulation was substantial enough to where (in an extreme example) the

overstrengthened anchor set with the best reliability after 20 generations in an optimization test proceeds to have the fourth-worst reliability in the 21st generation of the same test.

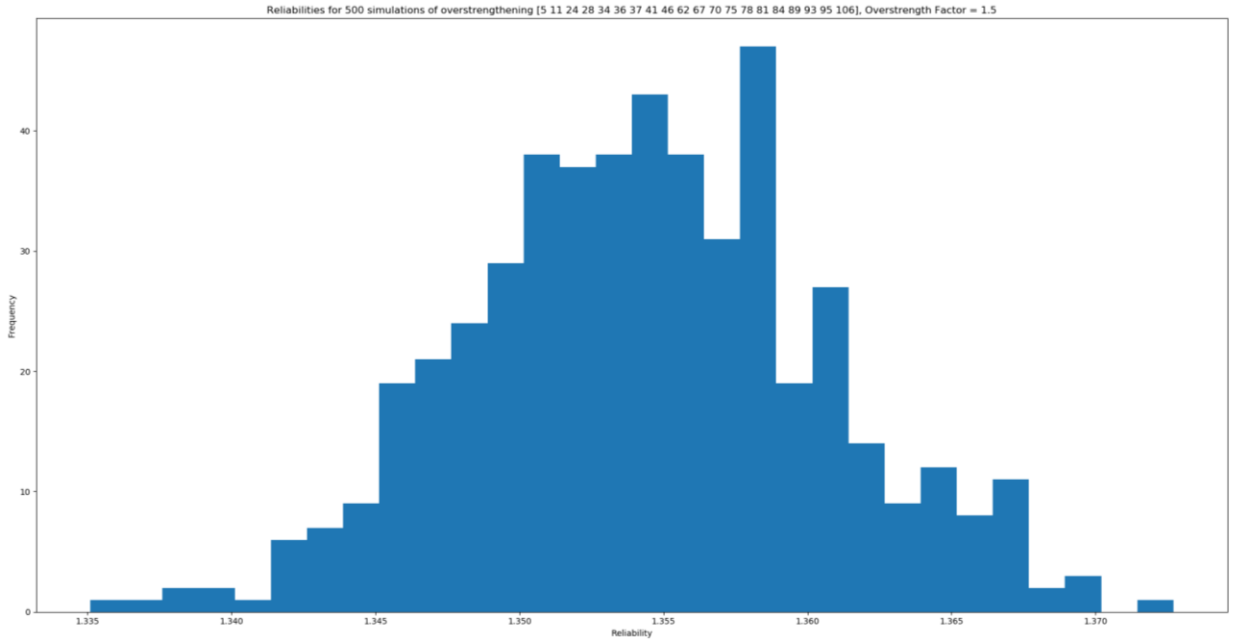


**Figure 5.** Histogram showing the reliability vs. frequency of a single set of overstrengthened anchors evaluated 500 times.

## 4.2 Final Results

One of the first notable results discovered was the behavior of the overstrength factor. As the overstrength factor was an algorithm parameter instead of an optimization variable, the optimization algorithm was simply run multiple times with varying overstrength factors and a varying number of overstrengthened anchors.

As shown in Figure 6, the lower overstrength values implicated reduced reliability, with the lowest overstrength factor of 1.1 diverging even at very low numbers of overstrengthened anchors, and 1.2 showing very little increase in reliability value if operating on more than five overstrengthened anchors. However, increasing the overstrength factor beyond 1.3 only gives marginal improvement in reliability, regardless of the number of overstrengthened anchors. It

appears that the reliability for a 1.3 overstrength factor begins to separate itself from higher overstrength factors beginning after 15 overstrengthened anchors, although this was not further tested due to the majority of the testing for this problem being constrained to 10 overstrengthened anchors. As such, the overstrength factor was set to 1.3 for all optimization tests.

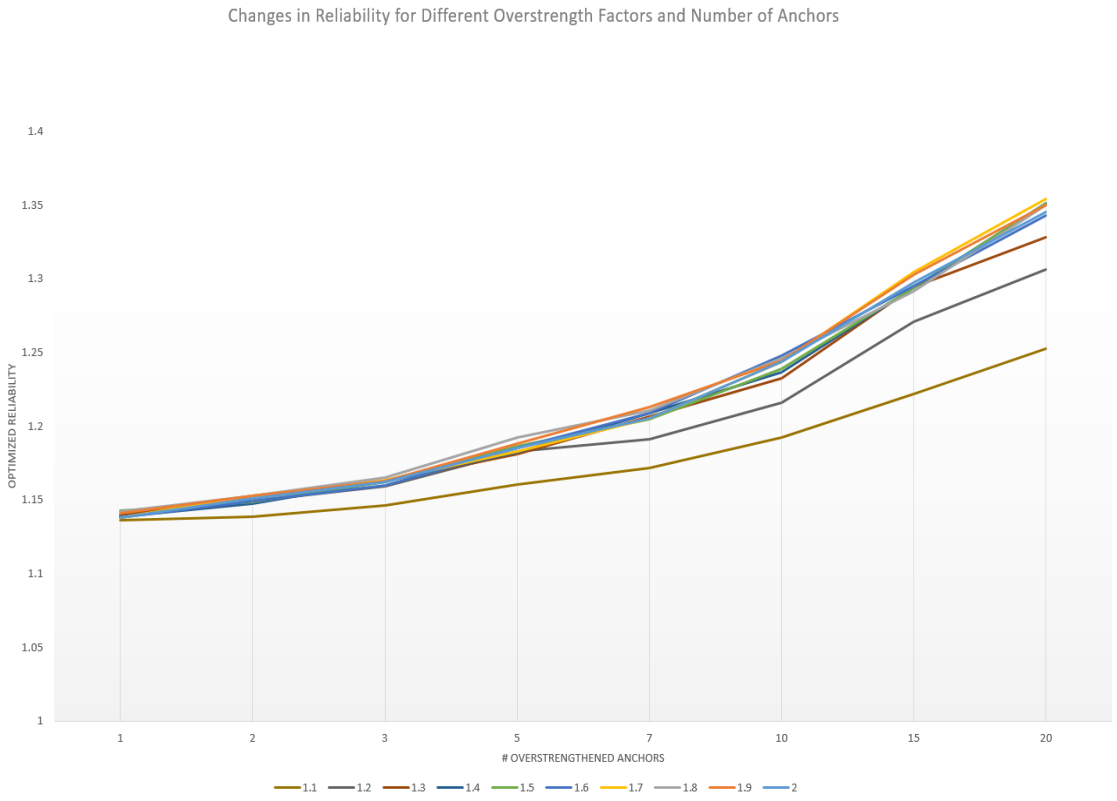


**Figure 6.** Number of overstrengthened anchors vs. optimized reliability for overstrength factors ranging 1.1 to 2.

With the addition of the Bayesian optimization and archiving, convergence to an optimal fitness level was achieved, though multiple optimal solutions were found. Specifically, reliability values converged to an optimal value of 1.2315 ± 0.0005, but the selected set of overstrengthened anchors would be somewhat different every time the algorithm converged on this reliability value. An example of this through eight tests of the optimization algorithm is shown in Table 4.

**Table 4.** Results of eight successful optimization attempts.

| **Optimization Test Results – 10 Overstrengthened Anchors, 1.3 OSF** | | |
|---|---|---|
| Optimization Test | Reliability | Overstrengthened Anchors |
| 1 | 1.2312 | 23 38 48 51 56 61 69 80 89 92 |
| 2 | 1.231 | 13 23 35 48 56 67 71 89 91 93 |
| 3 | 1.2319 | 23 27 49 51 56 73 78 83 90 92 |
| 4 | 1.232 | 23 36 40 56 59 60 68 83 89 92 |
| 5 | 1.232 | 9 34 36 51 56 70 72 78 89 94 |
| 6 | 1.231 | 5 34 47 56 59 73 78 83 89 92 |
| 7 | 1.2313 | 27 34 45 48 67 69 71 89 93 95 |
| 8 | 1.2311 | 9 23 39 45 56 70 73 78 93 100 |

These eight results were then charted simultaneously on a mapped wind farm layout, with different colors representing the number of times a specific anchor was selected across all optimization tests, functioning as a heat map. The results of this are shown in Figure 7.

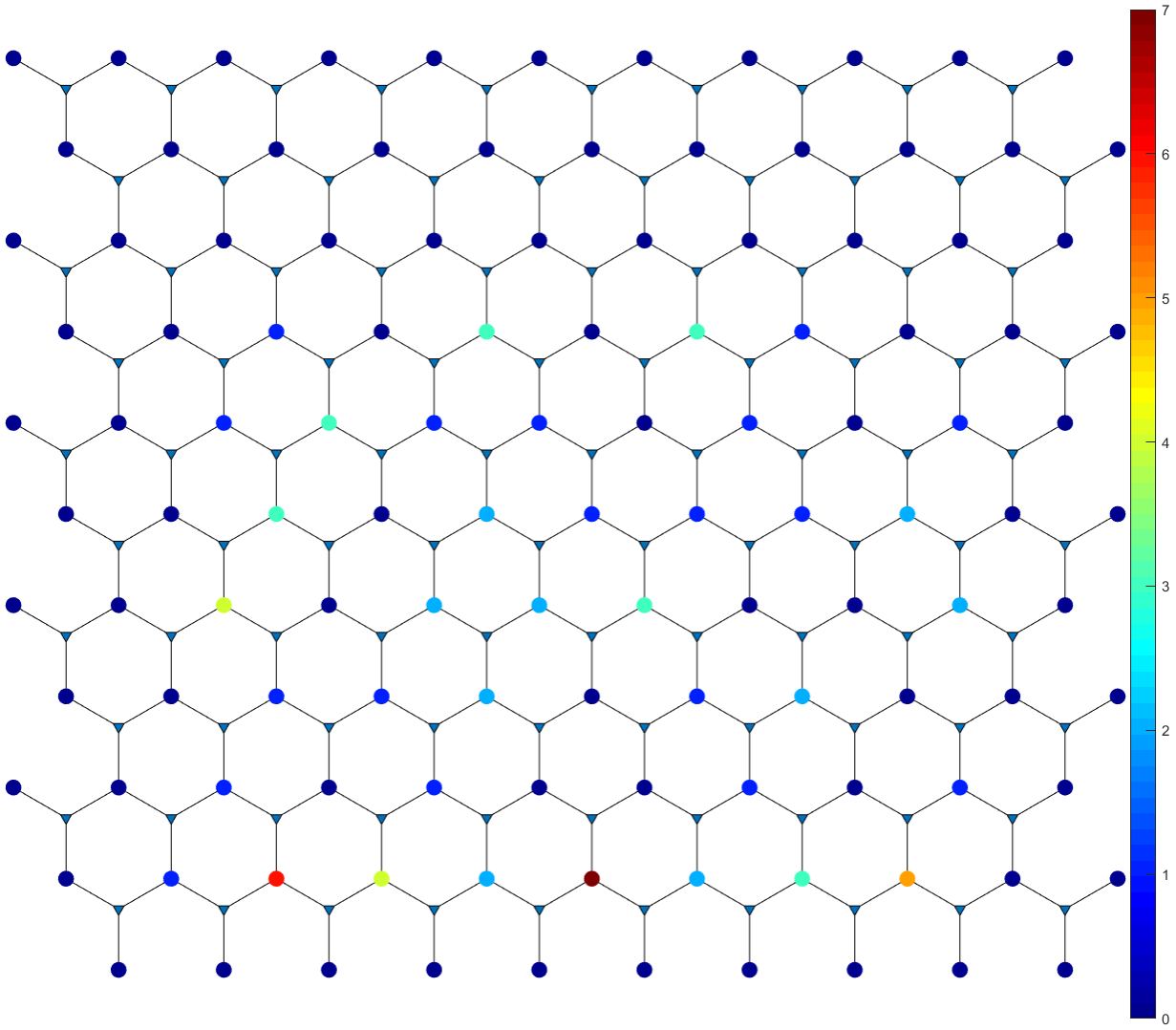


**Figure 7.** Heat map of the analyzed wind array, illustrating the frequency of selected overstrengthened anchors from the eight successful optimization tests in Table 4.

Upon analysis, there appears to be a moderate correlation between specific regions and the overstrengthening of anchors, as highlighted in Figure 8.

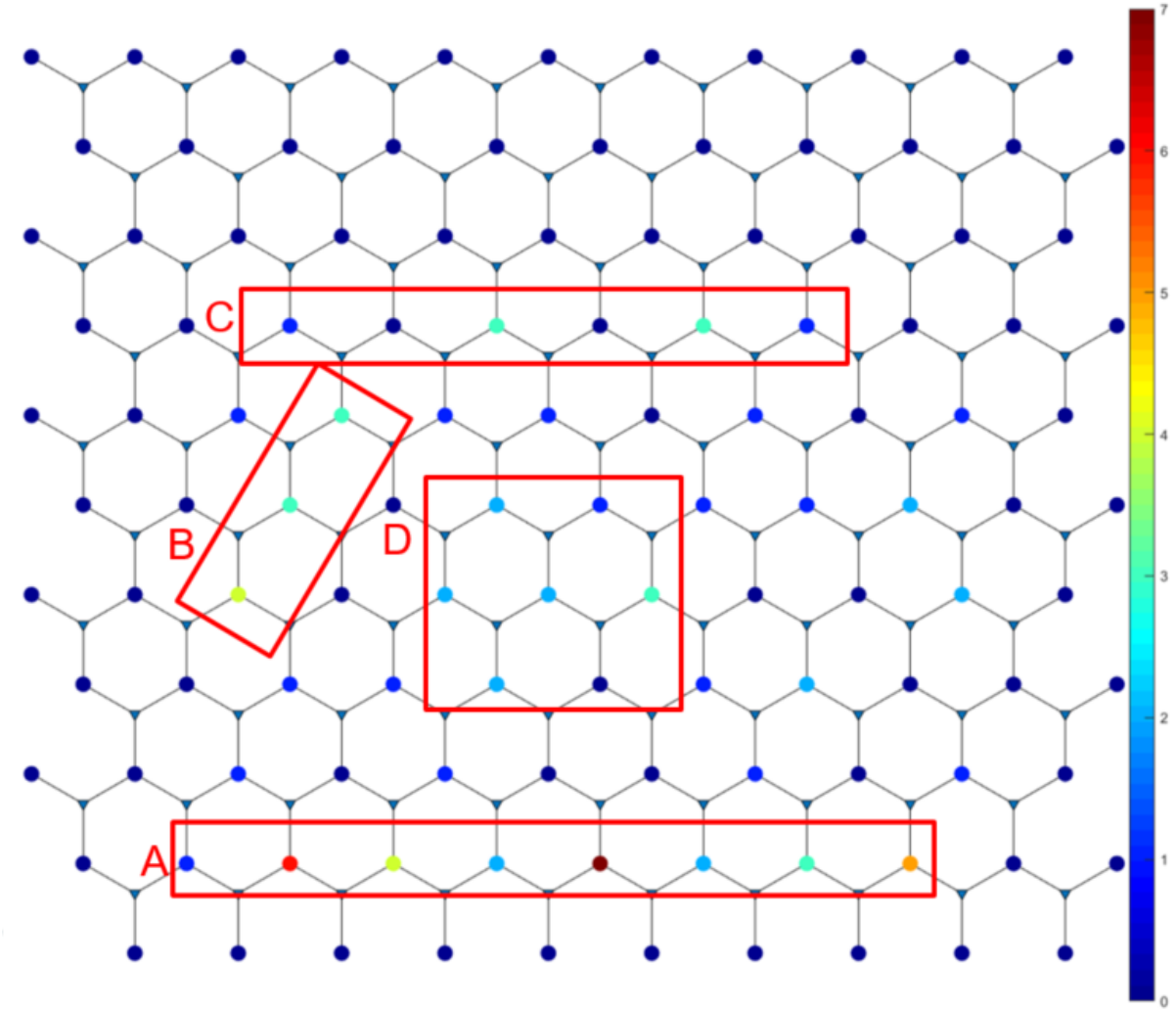


**Figure 8.** Heat map of the analyzed wind array, with boxes enclosing noteworthy regions.

The highlighted areas are as follows:

- Region A is the southernmost row in the array with multiline anchors. At least three anchors are always overstrengthened in every optimized array. The selected overstrengthened anchors are frequently spread out from east to west rather than being concentrated at any one section of the row.

- Region B is a set of three diagonal anchors in the central-west of the array. At least one of these anchors is overstrengthened in every optimized array. If two of the anchors were overstrengthened, it would be the top and bottom anchor in the region, never two adjacent anchors.
- Region C is the center part of the fourth northernmost row in the array. With one exception, every optimized array had at least one overstrengthened anchor in this region. Overstrengthened anchors also never appeared above this row.
- Region D is a hexagonal region of 7 anchors located slightly south of the center of the array. 1 to 3 anchors in this region were always overstrengthened in every optimized array. If multiple anchors were selected in this region, adjacent anchors were rarely selected.

Interestingly, with one exception (see Figure 9 below), nine of the 10 overstrengthened anchors would always fall within these four regions; there always is one overstrengthened anchor that falls in some other location in the array. This is likely a coincidence within the results rather than an indication of a specific behavior.

Figures 9 and 10 show two examples of optimized arrays, with a layover of the specified regions of interest. Note that Figure 9 provides several exceptions to several correlations discussed above.

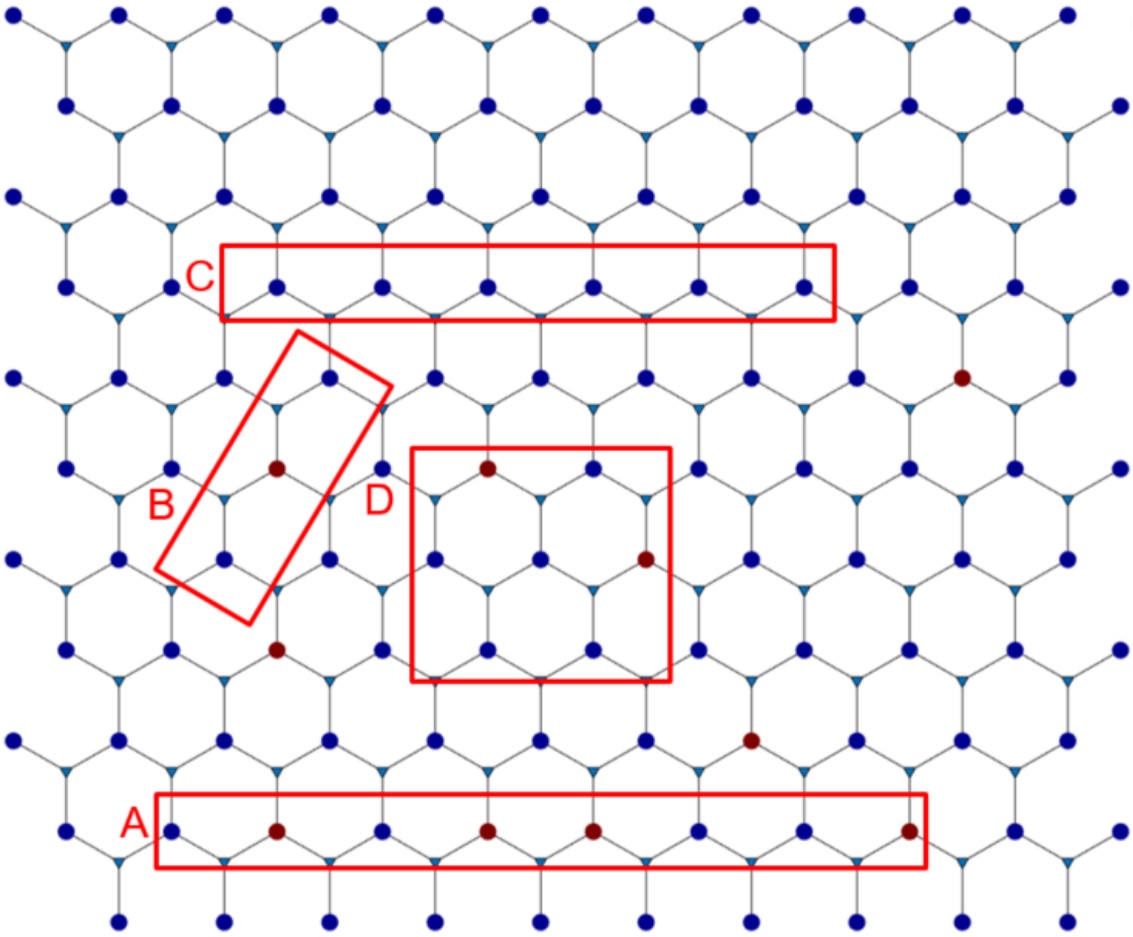


**Figure 9.** Optimized solution for 10 overstrengthened anchors, with some deviation from observed trends, 1.3 overstrength factor.

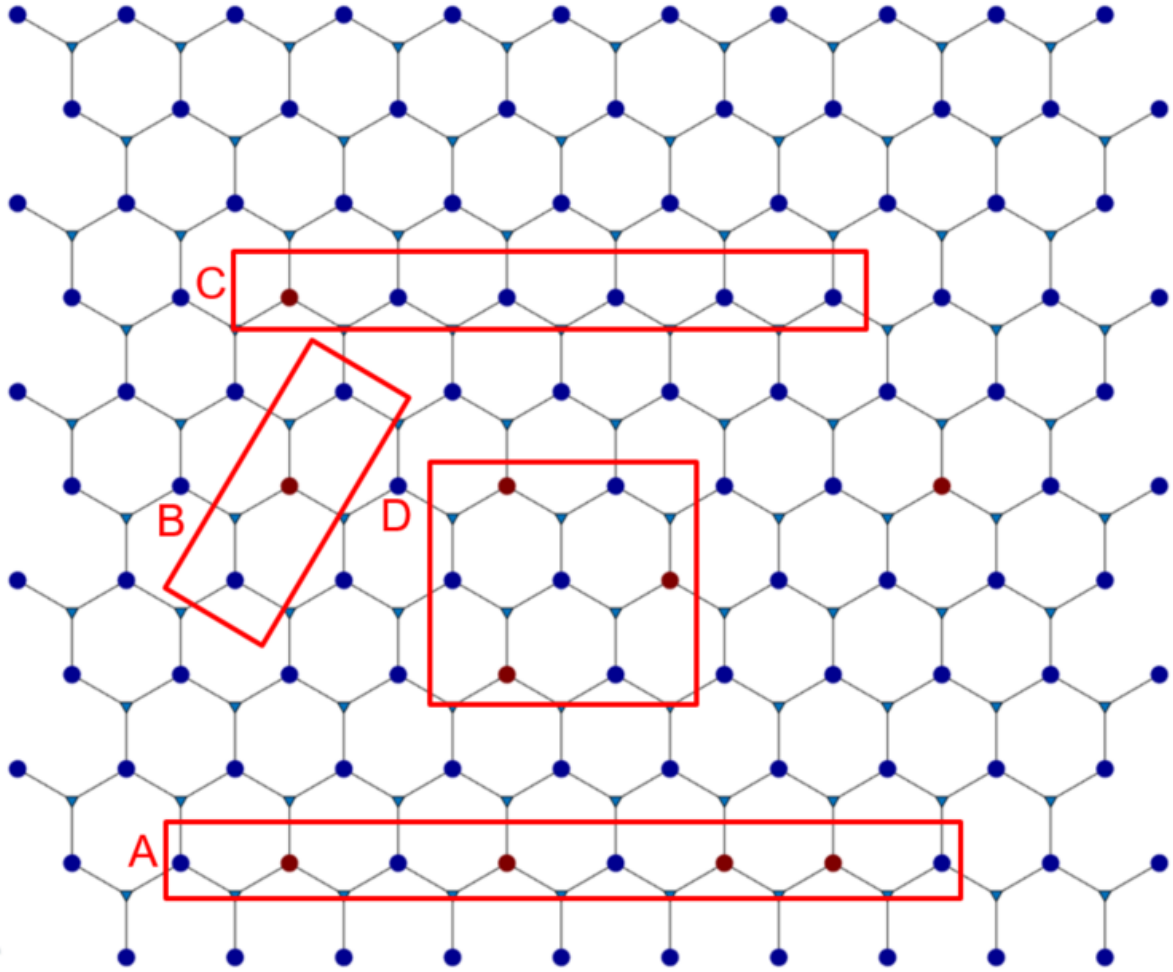


**Figure 10.** Optimized solution for 10 overstrengthened anchors, with adherence to observed trends, 1.3 overstrength factor.

While many of the aforementioned regions and trends are only moderately correlated, there appear to be three strong correlations:

1. Region A has the highest concentration of overstrengthened anchors
2. The southern half of the array has a higher concentration of overstrengthened anchors than the northern half
3. The “center of mass” of all overstrengthened anchors falls close to the central column

To further test the behavior of the anchor selection, the optimization algorithm was tested with overstrengthening three anchors and 30 anchors. The results from these optimization tests are shown in Figures 11 and 12.

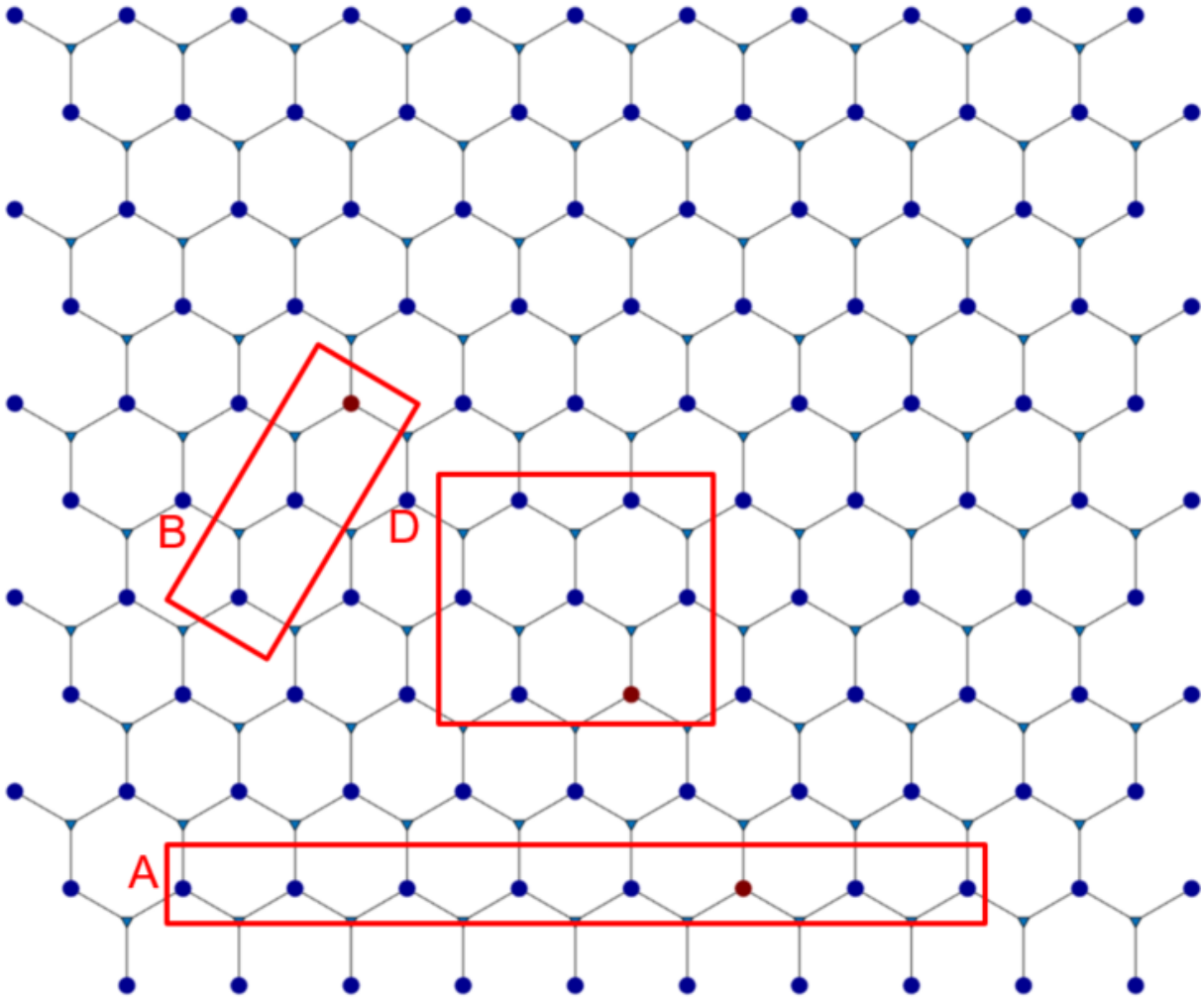


**Figure 11.** Optimized solution for three overstrengthened anchors, 1.3 overstrength factor.

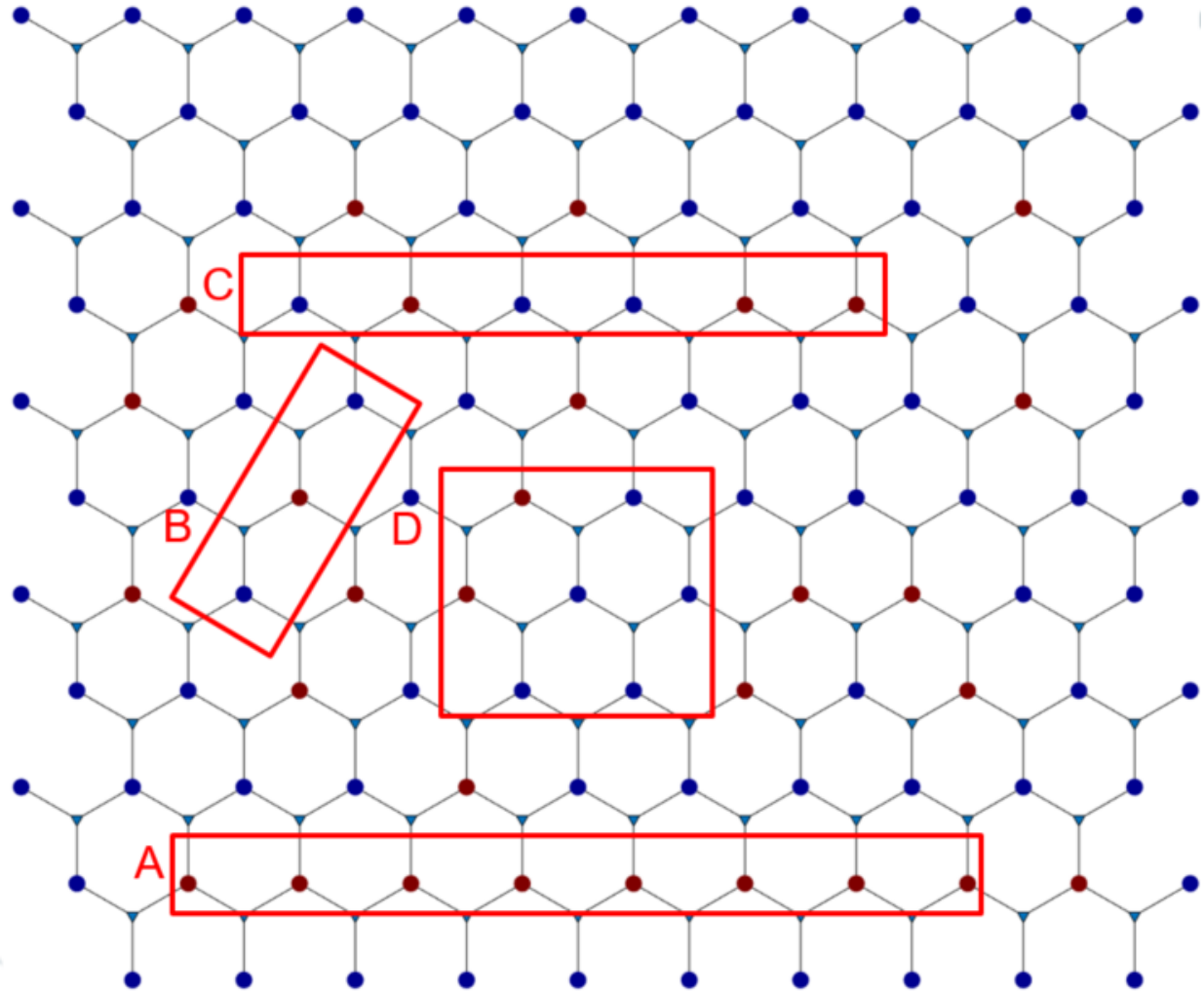


**Figure 12.** Optimized solution for 30 overstrengthened anchors, 1.3 overstrength factor.

Overall, the same strong correlations found in the tests with 10 overstrengthened anchors also appear in the tests with three and 30 overstrengthened anchors. As shown in Figure 11, one overstrengthened anchor falls within each of Regions A, B, and D. for the test with three overstrengthened anchors. In Figure 12, every anchor in Region A is overstrengthened, and the concentration towards the southern half of the array still holds true, while maintaining east-west symmetry.

Despite a single optimized configuration not being identified, the rationale behind the trends for the selection of overstrengthened anchors offers insight into which anchors to target in

the design of an array utilizing this multiline anchor theory. The concentration of overstrengthened anchors in the southern half of the array – especially in Region A – is likely due to the wind and wave forces acting on the array coming from the south. If an anchor in the southern part of the array fails, the coupling of the turbines and anchors makes it more likely for a single failure to lead to cascading failures than if an anchor in the north fails. As discussed by Arwade et al., this has the highest impact for multiline anchors near the edge of the array, explaining why Region A sees the highest concentration of overstrengthened anchors [26].

## 4.3 Comparison to Original Hypothesis

Once a convergent solution was identified, the resulting reliabilities from the optimization scheme were compared to the reliabilities of the same FOWT array where the strength of all anchors is increased to a lesser degree. The latter was acquired by testing the same simulation initially given (only all 120 array anchors were "overstrengthened") 500 times per overstrength factor and taking the mean reliability. The results of these tests are listed in Figure 13.

Optimization

| Anchors Strengthened to 1.3 OSF | Reliability |
|---|---|
| 3 | 1.151 |
| 10 | 1.2315 |
| 30 | 1.49676 |

Comparison Experiment

| Overstrength Factor | Reliability |
|---|---|
| 1 | 1.1088 |
| 1.025 | 1.3216 |
| 1.05 | 1.518 |
| 1.075 | 1.6969 |
| 1.1 | 1.8638 |
| 1.125 | 2.0194 |
| 1.15 | 2.1624 |
| 1.175 | 2.3008 |
| 1.2 | 2.428 |

**Figure 13.** Reliability comparison between optimization tests and comparison test with all anchors overstrengthened.

Even when anchors are optimized, the reliability from strengthening all anchors quickly surpasses the reliability for only overstrengthening a small number of anchors. This suggests the reliability of a FOWT array using this multiline concept is much more closely tied to the number of anchors strengthened than which anchors are strengthened, or by how much. Notably, the reliability value for the optimization test with 30 overstrengthened anchors appears substantially more competitive with the mass strengthening reliabilities. Drawing from this, it is possible there is a point where overstrengthening some larger number of optimized anchors (more than 30, less than 120) provides increased benefit over increasing the overall anchor strength, and optimizing the anchors for that scenario could lead to some credence to the original hypothesis. The number and optimized location of these anchors, as well as the cost-benefit analysis of this concept

versus simply strengthening all of the anchors to a lesser amount, is an area of substantial interest in future research.

# Chapter 5: Conclusion and Future Work

Floating offshore wind provides a substantial untapped supply of energy that can be utilized to meet increasing energy demand in the United States. However, the substantial costs associated with floating offshore wind prevent it from currently being commercially viable, and design optimization is required for the floating offshore wind to approach viability. A method has been proposed to decrease the cost of anchoring by connecting mooring lines from multiple turbines to a single anchor, substantially reducing the cost of the anchors for a large farm. My proposed hypothesis was that a high system reliability level could be maintained for such an array by strengthening the most important anchors more than the majority of the anchors in the array. Optimization was required to determine the best anchors to strengthen.

The simulation used to evaluate the reliability of a hypothetical floating wind array uses data from prior FAST analyses to determine the mean number of turbine and anchor failures that would result from the loading scenario specified by the user, as detailed in section 3.2. A binary genetic algorithm was initially attempted as a means to maximize the reliability of the simulation for a preset number of overstrengthened anchors and an overstrength factor, but this optimization algorithm proved to be sensitive to noisy evaluations resulting from probabilistic sampling within the provided simulations, and failed to converge as a result. To counter this, aspects of Bayesian optimization, such as treating repeated evaluations as a Gaussian process prior, made the optimization algorithm resistant to noise and succeeded in converging to a single reliability value, albeit with many optimal solutions.

As discussed in Chapter 4, the resulting configurations from optimized arrays show selected overstrengthened anchors being concentrated in the direction of wind and wave forces, due to the effects of cascading failures if these components fail. However, optimizing and significantly strengthening a small number of anchors failed to match the reliability of slightly strengthening all array anchors, though the results suggest overstrengthening a much larger number of anchors in optimized locations could still provide substantial benefits to the overall reliability of the system.

Future work will entail identifying the relation between the number of optimized anchors and the reliability for a much larger set of overstrengthened anchors, and identifying if there is a point where the optimized overstrengthening method provides greater benefit than simply overstrengthening all array anchors. The explicit costs of these two options – particularly the potential savings to the construction of a large floating offshore wind farm – also warrants future investigation.

# Works Cited

[1] U.S. Energy Information Administration, "Annual Energy Outlook 2017," U.S. Department of Energy, Washington, 2017.

[2] M. Schwartz, D. Heimiller, S. Haymes and W. Musial, "Assessment of Offshore Wind Energy Resources for the United States," National Renewable Energy Laboratory, Golden, CO, 2010.

[3] National Renewable Energy Laboratory, "Wind resource estimates developed by AWS Truepower, LLC," 15 June 2016. [Online]. Available: http://www.nrel.gov/gis/images/80m_wind/awstwspd80onoffbigC3-3dpi600.jpg. [Accessed 27 February 2019].

[4] GWEC, "Offshore Wind," GWEC, 2018.

[5] NOAA, "Pacific Coast Nautical Chart," 2018. [Online]. Available: https://charts.noaa.gov/Catalogs/pacific_chartside.shtml. [Accessed 27 February 2019].

[6] J. S. Hill, "Hywind Scotland, World's First Floating Wind Farm, Performing Better Than Expected," Sustainable Enterprises Media, Inc., 16 February 2018. [Online]. Available: https://cleantechnica.com/2018/02/16/hywind-scotland-worlds-first-floating-wind-farm-performing-better-expected/. [Accessed 27 Februrary 2019].

[7] R. James and M. C. Ros, "Floating Offshore Wind: Market and Technology Review," The Carbon Trust, Edinburgh, 2015.

[8] C. Molins, P. Trubat, X. Gironella and A. Campos, "Design Optimization for a Truncated Catenary Mooring System for Scale Model Test," *Marine Science and Engineering,* vol. 3, pp. 1362-1381, 2015.

[9] M. Brommundt, L. Krause, K. Merz and M. Muskulus, "Mooring system optimization for floating wind turbines using frequency domain analysis," *Energy Procedia,* vol. 24, pp. 289-296, 2012.

[10] D. Chen, P. Gao, S. Huang, K. Fan, N. Zhuang and Y. Liao, "Dynamic response and mooring optimization of spar-type substructure under combined action of wind, wave, and current," *Renewable and Sustainable Energy,* vol. 9, no. 6, p. 063307, 2017.

[11] G. Benassai, A. Campanile, V. Piscopo and A. Scamardella, "Optimization of Mooring Systems for Floating Offshore Wind Turbines," *Coastal Engineering,* vol. 57, no. 4, pp. 1550021-1 - 1550021-19, 2015.

[12] I. Fylling, "Optimization of Mooring and Riser System for Deep Water Floating Production Systems Including Fatigue Life Requirements," in *International Symposium on Deepwater Mooring Systems*, Houston, 2003.

[13] I. Fylling and P. A. Berthelsen, "WINDOPT - An optimization tool for floating support structures for deep water wind turbines," in *OMAE2011*, Rotterdam, 2011.

[14] M. Hall and A. Goupee, "Validation of a lumped-mass mooring line model with DeepCwind semisubmersible model test data," *Ocean Engineering,* vol. 104, pp. 590-603, 2015.

[15] M. Hall, B. Buckham and C. Crawford, "Evaluating the importance of mooring line model fidelity in floating offshore wind turbine simulations," *Wind Energy,* vol. 17, pp. 1835-1853, 2014.

[16] G. Vissio, B. Passione, M. Hall and M. Raffero, "Expanding ISWEC Modelling with a Lumped-Mass Mooring Line Model," in *EWTEC2016*, Nantes, 2015.

[17] S. Sirnivas, M. Hall, Y.-H. Yu and B. Bosma, "Coupled mooring analyses for the WEC-Sim wave energy converter design tool," in *OMAE 2016*, Busan, 2016.

[18] M. Hall, "Efficient modelling of seabed friction and multi-floater mooring systems in MoorDyn," in *EWTEC2017*, Cork, 2017.

[19] P. Connolly and M. Hall, "Comparison of pilot-scale floating offshore wind farms with shared moorings," *Ocean Engineering,* vol. 171, pp. 172-180, 2019.

[20] M. Goldschmidt and M. Muskulus, "Coupled mooring systems for floating wind farms," *Energy Procedia,* vol. 80, pp. 255-262, 2015.

[21] C. M. Fontana, D. J. DeGroot, M. Landon, S. R. Arwade, A. T. Myers and C. Aubeny, "Efficient multiline anchor systems for floating offshore wind turbines," in *OMAE 2016*, Busan, 2016.

[22] R. P. Adams, "A Tutorial on Bayesian Optimization for Machine Learning," 14 August 2014. [Online]. Available: https://www.iro.umontreal.ca/~bengioy/cifar/NCAP2014-summerschool/slides/Ryan_adams_140814_bayesopt_ncap.pdf. [Accessed 24 February 2019].

[23] P. I. Frazier, "A Tutorial on Bayesian Optimization," 10 July 2018. [Online]. Available: https://arxiv.org/pdf/1807.02811.pdf. [Accessed 22 Februrary 2019].

[24] A. Gruber and I. Ben-Gal, "Efficient Bayesian Network Learning for System Optimization in Reliability Engineering," *Quality Technology & Quantitative Management,* vol. 9, no. 1, pp. 97-114, 2012.

[25] S. T. Hallowell, S. R. Arwade, C. M. Fontana, D. J. DeGroot, C. P. Aubeny, B. D. Diaz, A. T. Myers and M. E. Landon, "System reliability of floating offshore wind farms with multiline anchors," *Ocean Engineering,* vol. 160, pp. 94-104, 2018.

[26] S. Arwade and S. Hallowell, Interviewees, *Mooring and Anchoring Optimization.* [Interview]. 20 February 2018.